ACS Pharmacology & Translational Science

pubs.acs.org/ptsci

Article

Prolyl Hydroxylase Domain Protein Inhibitor Not Harboring a 2-Oxoglutarate Scaffold Protects against Hypoxic Stress

Kento Sonoda, Sudarma Bogahawaththa, Akito Katayama, Saki Ujike, Sae Kuroki, Naho Kitagawa, Kohichi Hirotsuru, Norio Suzuki, Toshio Miyata, Shin-ichi Kawaguchi, and Tadayuki Tsujita*

Cite This: *ACS Pharmacol. Transl. Sci.* 2022, 5, 362−372

Read Online

ACCESS | Metrics & More | Article Recommendations | Supporting Information

ABSTRACT: Hypoxia-inducible factor-α (HIF-α) activation has shown promising results in the treatment of ischemia, such as stroke, myocardial infarction, and chronic kidney disease. A number of HIF-α activators have been developed to improve the symptoms of these diseases. Many feature 2-oxoglutarate (2-OG) scaffolds that interact with the active centers of prolyl hydroxylase domain-containing proteins (PHDs), displacing the coenzyme 2-OG. This stabilizes HIF-α. Therefore, the specificity of the 2-OG analogs is not high. Here, we identified 5-(1-acetyl-5-phenylpyrazolidin-3-ylidene)-1,3-dimethylbarbituric acid (PyrzA) among over 10 000 compounds as a novel HIF activator that does not contain a 2-OG scaffold. In cultured cells, PyrzA enhanced HIF-α stability and upregulated the expression of HIF target genes. Interestingly, PyrzA decreased HIF-1α prolyl hydroxylation, suggesting that PyrzA may activate HIF to prevent the degradation of HIF-α. These results indicate that PyrzA stabilizes HIF via a novel mechanism and could be a potential HIF activator candidate.

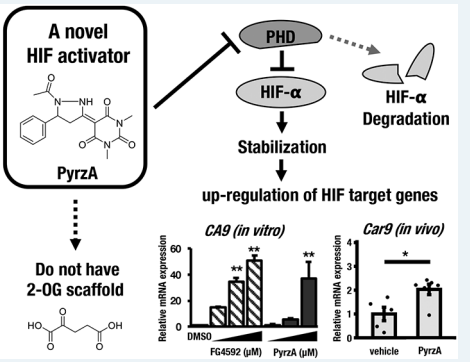

KEYWORDS: *PHD inhibitor, hypoxic stress, hypoxia inducible factor, pyrazolidine, erythropoietin*

A sufficient amount of molecular oxygen (O_2) must be delivered to the peripheral tissues to create adenosine triphosphate through the cellular respiration pathway. In live cells and/or organisms, lowering the O_2 concentration leads to severe stress. To date, the formation of microclots in capillary vessels has been reported to induce hypoxic stress, which is an initial event for stroke, heart failure, and kidney diseases.[1−3] To prevent the progression of these diseases, the upregulation of hypoxia-protective proteins, such as vascular endothelial growth factor (VEGF), erythropoietin (EPO), and glucose transporter 1 (GLUT1), potentiates cells to modify metabolic features in response to a hypoxic condition.[1,4−6] Not only do these proteins have strong feasibility for rescuing hypoxic stress, but they also have a side effect of assisting the malproliferation activity of certain cancer cells.[5,7−10] Therefore, these hypoxia response mechanisms should be controlled and made reversible if they are to be used to treat hypoxia-related diseases. For this reason, academic researchers and pharmaceutical companies have been working on exploring small molecular compounds that can activate the hypoxia sensing system without exposing the low oxygen condition.[11−13]

Transactivation with hypoxia-inducible factors (HIFs) is an indispensable event in protecting against hypoxic stress through the hypoxia protective proteins mentioned above.[14−16] HIF-1 belongs to the PER-ARNT-SIM (PAS) subfamily of the basic helix−loop−helix (bHLH) family of transcription factors. HIFs are divided into two major subfamilies: those with the unstable alpha subunit (HIF-α) and those with the stable beta subunit (HIF-β).[17,18] After forming the HIF α/β heterodimer, HIF has the potential to bind the hypoxia response element (HRE) ([A/G]CGTC) and transactivate the hypoxia target genes.[10,19] Under normal oxygen conditions (normoxia), HIF-α is continuously hydroxylated by prolyl hydroxylase domain-containing proteins (PHDs).[9,20,21] On HIF-α, PHDs recognize two proline residues called oxygen-dependent degradation domains (ODDs): one on the N-terminal side (NODD, Pro402) and the other on the C-terminal side (CODD, Pro564).[22] Conversely, hydroxylated HIF-α is caught by the von Hippel−Lindau protein (pVHL), which belongs to the E3 ubiquitin ligase complex.[23−27] This event leads to the polyubiquitylation of hydroxylated HIF-α, which leads to its degradation via the ubiquitin−proteasome system. Conversely, HIF-α hydroxylation is suppressed under hypoxic conditions due to a reduction in oxygen molecules. As a result, HIF-α stabilizes and translocalizes to the nucleus.

Received: January 5, 2022
Published: April 13, 2022

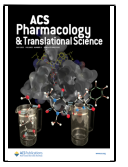

Although continuous HIF-α stabilization is beneficial in the treatment of ischemic injury, it affects broad tissues and causes unfavorable side effects such as neovascularization, plethora, and tumorigenesis.[8,28,29] For the proof-of-concept of these achievements, tissue-specific PHD1 or PHD2 knockout mice have been developed. Only PHD2 knockout mice, but not PHD1 or PHD3 knockout mice, died during the embryonic period.[28,30] In addition, polycythemia occurred more frequently in adult liver-specific PHD2 knockout mice than in PHD1 or PHD3 knockout mice.[31,32] Moreover, the PHD1−3 isoforms have shown differential sensitivity to the HIF-α isoforms.[33,34] In particular, HIF-1α and HIF-2α have shown changes in the tissues where they are expressed,[35−37] expression time,[38,39] and downstream target genes.[40−43] For example, HIF-1α suppresses tumorigenesis by inhibiting c-Myc transcriptional activity. Conversely, HIF-2α promotes tumorigenesis by enhancing c-Myc function.[38,44−46] As a result, partial and transient HIF-α stabilization strategies using chemical compounds have become attractive. This approach can target typical proteins, including HIF-α, PHDs, VHL, and protein−protein interfaces without exposing the cells to hypoxic conditions. In addition, one of the most beneficial aspects of using synthetic chemical compounds to activate HIF-α is the ability to control the duration, timing, tissue specificity, and delivery.

To stabilize the HIF-α protein with small chemical compounds, the inhibition of PHD enzyme activities has been a major point of focus. PHDs require ferrous ions (Fe^{2+}), 2-oxoglutarate (2-OG), and ascorbic acid to hydroxylate HIF-α ODD.[47,48] Competitive inhibitors derived from the 2-OG structure have been synthesized[11,12,49−51] and developed as new types of therapeutic compounds for renal anemia.[52−61] FG4592 (roxadustat), for example, was recently approved as a therapeutic compound for anemia associated with chronic kidney disease (CKD).[62,63] However, it is estimated that more than 60 proteins have 2-OG as a cofactor.[13,50,64] Therefore, the VHL inhibitor[65,66] and FIH inhibitor[67−71] have been developed as inhibitors targeting compounds other than PHDs without mimicking 2-OG; however, they have not yet been approved. Although a large number of PHD inhibitors have been reported, there are still several HIF activators that do not harbor the 2-OG scaffold.

In this study, we aimed to identify a novel structure-type HIF activator. To achieve this, we created a classic HRE-reporter system, which included a hypoxia response output event HIF activation reporter assay[72] as a black-box screening system from a broad range of chemical libraries. We found 5-(1-acetyl-5-phenylpyrazolidin-3-ylidene)-1,3-dimethylbarbituric acid (PyrzA)[73] as a hit compound using high-throughput screening (HTS). However, PyrzA is a novel chemical compound that has only been reported for its chemical structure, and there have been no official reports on its use. We demonstrated that PyrzA stabilizes both HIF-1α and HIF-2α in a dose-dependent manner by inhibiting PHDs and upregulating HIF target genes *in vitro* and *in vivo*. This study shows the discovery of a novel HIF inducer, PyrzA, and the possibility of different HIF activation mechanisms.

RESULTS AND DISCUSSION

Finding PyrzA as a Novel HIF-Inducing Compound through High-Throughput Screening. To find a broad range of HIF-α inducer compounds from a chemical library, we focused on monitoring the end point HIF-α transcriptional activity using a luciferase reporter system. Previously, we generated a nanoluciferase (NLuc) reporter system under control with seven tandem repeats of human VEGF HRE elements attached to a mini-TATA promoter. For HTS, the human neuroblastoma cell line SK-N-BE(2)-C (SKN) that stably harbored the construct SKN:HRE-NLuc was used.[72] The HTS criteria values including S/B, S/N, and Z′ factor for this HIF-α inducer screening system were 183, 1137, and 0.54, respectively. First, a total of 7.0×10^3 cells of SKN:HRE-NLuc were seeded into each well of a 384-well plate and stimulated with the core 9600 chemical library (final dose in 20 μM) from the Drug Discovery Initiative, University of Tokyo (DDI). The negative control was 1% (v/v) DMSO and the positive control was 100 μM $CoCl_2$. At 24 h after stimulation, the nano-Glo luciferase reagent was added directly, and HIF-α transcriptional activity was measured. The values were indicated with the percentile of the DMSO control average value (Figure 1A).

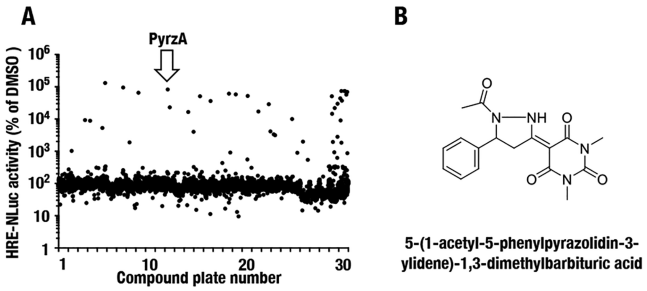

Figure 1. Identification of the unique HIF inducer, PyrzA, from a large chemical library. (A) The initial screening result from the core 9600 chemical library from the Drug Discovery Initiative, The University of Tokyo using with SKN:HRE-NLuc reporter cell line. SKN:HRE-NLuc cells (7.0×10^3 cells) were seeded into a 384-well plate and treated with the chemical compound library (20 μM each) for 24 h. The nano luciferase activity in each well was measured. The HIF reporter activity of each compound was calculated with the indicated with the % of nano luciferase activity of positive controls (100 μM $CoCl_2$) and indicated as an individual dot. The hit compound, PyrzA, is indicated with an open arrow. (B) The chemical structure of PyrzA: 5-(1-acetyl-5-phenylpyrazolidin-3-ylidene)-1,3-dimethylbarbituric acid.

Second, we selected 40 secondary hit compounds through serial dilution activity screening (data not shown). Third, compounds that were frequently hit, including known HIF activators such as dihydroxybenzene[74,75] and oxyquinoline,[76,77] and those having a 2-OG containing structure were removed from the candidate list. Eventually, we selected PyrzA (Figure 1B) from our initial hits (open arrow in Figure 1A).

Synthesis of PyrzA. Although PyrzA was included in the library, no method for its synthesis has been reported to date. Therefore, we first carried out the synthesis of PyrzA using the reaction conditions of a similar compound, 5-(1-acetyl-5-phenylpyrazolidin-3-ylidene), or barbituric acid, as in ref 78. However, the reaction conditions could not be adapted for the synthesis of PyrzA. Therefore, we attempted to synthesize the desired PyrzA in a two-step reaction using (*E*)-1,3-dimethyl-5-(3-phenylacryloyl)barbituric acid (**1**) as the starting material (Scheme 1). Among the several known methods for the synthesis of compound **1**, the method reported by Lejon et al. was the most effective.[79] The pyrazoline formation reaction was carried out using hydrazine and enone compounds under typical conditions[80] for the synthesis of **1** to **2**.

https://doi.org/10.1021/acsptsci.2c00002
ACS Pharmacol. Transl. Sci. 2022, 5, 362−372

Scheme 1. General Pathway for the Synthesis of 1,3-Dimethyl-5-(5-phenylpyrazolidin-3-ylidene)barbituric acid (2) and PyrzA (3)

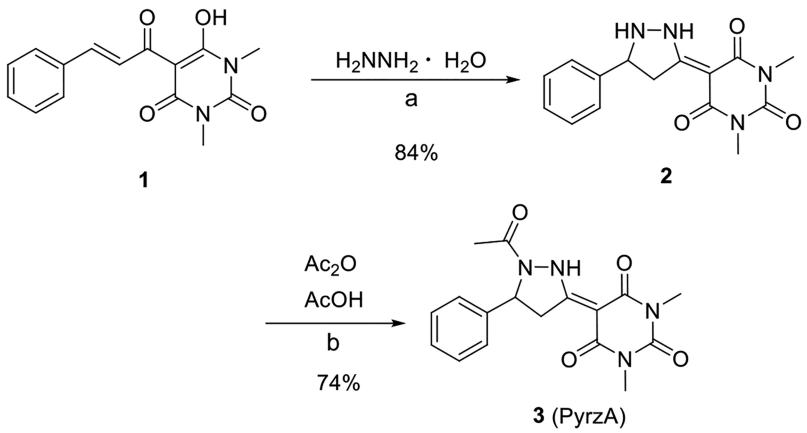

[a]Synthesis of compound **2**: (*E*)-1,3-dimethyl-5-(3-phenylacryloyl)barbituric acid (**1**), hydrazine monohydrate, ethanol, reflux, 1 h (84% for 2); [b]Synthesis of compound **3**: **2**, acetic acid, acetic anhydride 125 °C, 2 h (74% for **3**)

The ^{1}H and ^{13}C NMR measurements showed that there was no double bond in the five-membered ring structure of **2**. This favored the presence of a double bond in the bond connecting the barbituric acid skeleton to the nitrogen (N)-containing five-membered ring structure. This was also the case for compound **3**. Finally, acetylation of the N on the phenyl side of the pyrazolidine skeleton was carried out using acetic anhydride to obtain the desired compound **3**, PyrzA, in high yield. Because the N atom on the barbituric acid side of the two N atoms in the pyrazolidine ring could form a tautomeric structure with the structure of the barbituric acid side, the nucleophilicity was weak, and the acetylation of the N atom on the phenyl side of the pyrazolidine skeleton proceeded selectively (Scheme 2). From the NMR and MS results, the structure of the compound in the library was confirmed to be PyrzA, as shown in Figure 1B.

Scheme 2. Tautomeric Structure of 1,3-Dimethyl-5-(5-phenylpyrazolidin-3-ylidene)barbituric Acid (2)

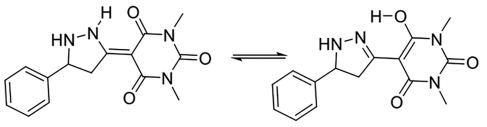

PyrzA Can Activate the HIF Signaling Pathway in a Dose- and Time-Dependent Manner. To compare PyrzA with dimethyloxalylglycine (DMOG) and FG4592, HIF reporter activities and cellular toxicities of these chemicals were measured using SKN:HRE-NLuc. DMOG and FG4592 have been approved as PHD inhibitors in the subclinical stage. FG4592 has also been approved for the treatment of anemia intervention. First, SKN:HRE-NLuc cells were treated with a series of diluted PyrzA, DMOG, or FG4592 for 24 h. The HIF transcriptional activity and cellular viability were measured using NLuc activity and the cell counting kit-8 (CCK-8) using WST-8 (2-(2-methoxy-4-nitrophenyl)-3-(4-nitrophenyl)-5-(2,4-disulfophenyl)-2*H*-tetrazolium), respectively (Figure 2A). The HIF activity for PyrzA, DMOG, or FG4592 was shown with a NLuc ratio of a 1% DMSO value as 1.0 (Figure 2B–D, left-side *y*-axis). The cell viability for these three chemicals was also indicated as the percentile ratio for 1% DMSO value as 100% in the right-side *y*-axis (Figure 2B–D, right-side *y*-axis). All three chemicals activated the HRE NLuc reporter in a dose-dependent manner. The DMOG, FG4592, and PyrzA concentrations for 5-fold HRE NLuc reporter activity were 6.78, 2.51, and 7.34 μM, respectively. None of the three chemicals showed cellular toxicity, even at the highest concentration (100 μM). These results indicated that PyrzA had a similar HIF activation potential to that of DMOG.

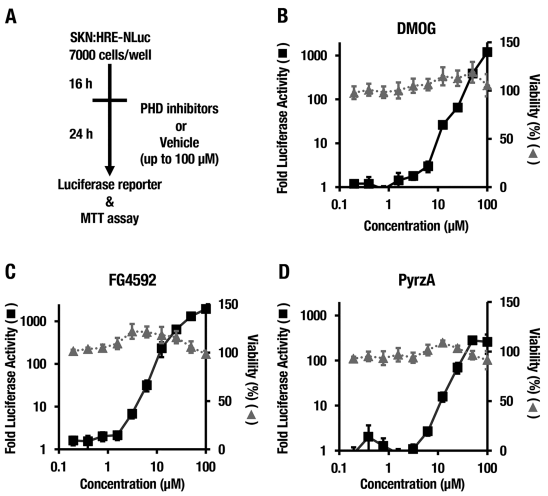

Figure 2. PyrzA can activate HRE reporter in a dose dependent manner without exhibiting toxicity. (A) Experimental procedure to evaluate for HIF-α transcriptional activity and cellular viability. (B–D) HIF-α transcriptional activity and cellular viability results for DMOG (B), FG4592 (C), or PyrzA (D) using SKN:HRE-NLuc for 24 h. The HRE reporter activities are indicated as fold luciferase activity, based on the value from 1% DMSO treated cells (filled square and solid line). The cell viability percentile is represented on the value from 1% DMSO treated cells as 100% viability (filled triangle and dashed line).

PyrzA Stabilizes HIF-α Protein under Normoxic Conditions. HIF-α consists of two isoforms: HIF-1α and HIF-2α. To confirm the stabilization of these proteins, we conducted an immunoblot analysis in several cell lines. SKN, HeLa, and Hep3B cells have already reported HIF stabilization with several HIF activators, including a PHD inhibitor

https://doi.org/10.1021/acsptsci.2c00002
ACS Pharmacol. Transl. Sci. 2022, 5, 362–372

containing a 2-OG structure. Before chemical challenging, 5.0 × 10^5 cells were seeded into each well of 12-well plates and preincubated for 16 h. After incubation, the cells were challenged with PyrzA or FG4592 at concentrations up to 100 μM for 24 h and the negative control vehicle, DMSO. The results showed that treatment with PyrzA or FG4592 led to dose-dependent stabilization of HIF-1α in SKN, HeLa, and Hep3B cells (Figure 3A, B, and C, respectively). Importantly, a

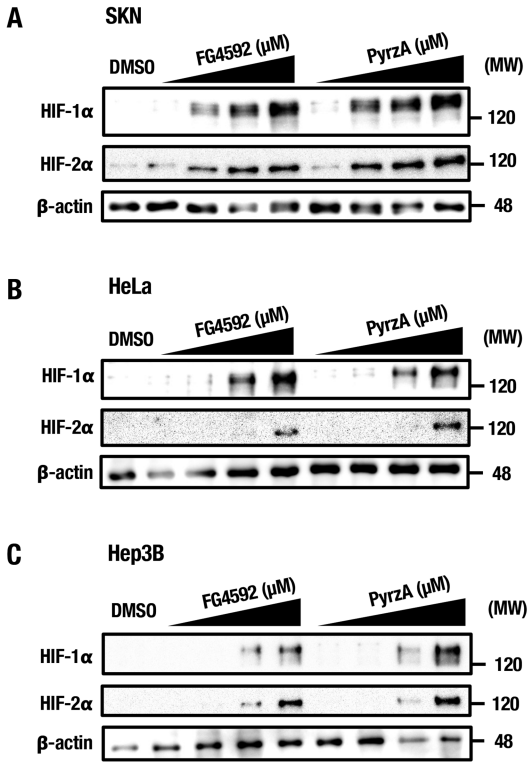

Figure 3. PyrzA stabilizes HIF-α protein in various cell lines. (A–C) Immunoblot analyses of HIF-α during various concentrations (1.0, 5.0, 25, and 100 μM) of PyrzA and target positive control, FG4592, in SKN (A), HeLa (B), and Hep3B (C) cells. Total cellular extract was separated by SDS-PAGE and transferred to PVDF membrane prior to treatment with appropriate antibodies. Lane 1 shows a negative DMSO vehicle control. Equal loading was assessed by probing the blots with antibody against β-actin. All of experiments were performed in triplicate, representative data are shown.

comparison of FG4592 and PyrzA on the same blot showed that the amount of HIF-α with PyrzA was the same as that with FG4592 in the three cells. These results suggest that PyrzA stabilizes HIF-α and the approved PHD inhibitor, FG4592.

PyrzA Stabilizes the HIF-α Protein by Inhibiting HIF-α Prolyl Hydroxylation. Under normoxic conditions, two prolyl residues, NODD and CODD, on HIF-1α (Pro402 and Pro564 in humans, respectively) were hydroxylated by PHD activity. The resultant hydroxylated form of HIF-1α was ubiquitinated by the VHL complex. The ubiquitinated HIF-1α was degraded via the ubiquitin-proteasome system. Because most of the known HIF activators target the 2-OG HIF-α prolyl hydroxylation epicenter in PHDs, we focused on whether the prolyl motif in HIF-1α was hydroxylated. To stabilize the HIF-α protein before ubiquitin-proteasome degradation, we checked the toxic effects of the proteasome inhibitor, MG132, in SKN, HeLa, and Hep3B cells. The three cell types were treated with serial dilutions of MG132 for 24 h, and the cell viability was analyzed using CCK-8. The LD_{50} of MG132 in all three cell lines was over 10 μM (data not shown). However, the majority of the Hep3B cells showed ballooning features during treatment with high concentrations of MG132; therefore, we decided not to use Hep3B to check the inhibitory activity of HIF-α prolyl hydroxylation by PyrzA and FG4592. To stabilize the HIF-1α protein, we set the MG132 concentration at 10 μM to partially inhibit the proteasomal activity. As shown in Figure 3, 5.0 × 10^5 SKN and HeLa cells were challenged with various doses of PyrzA or FG4592 (1, 5, 25, and 100 μM). The cells were treated with 10 μM MG132 for 24 h to investigate the hydroxylation of HIF-1α prior to degradation. Two hydroxylation sites on HIF-1α, including Pro402 and Pro564, were detected with hydroxylation-specific antibodies. In SKN and HeLa cells, only PyrzA or FG4592 treatment stabilized the HIF-1α protein. MG132 treatment also stabilized the HIF-1α protein in SKN and HeLa cells.

PyrzA or FG4592 treatment blocked the Pro402 and Pro564 hydroxylation of HIF-1α in SKN and HeLa cells in a dose-dependent manner (Figure 4A and B, respectively). Notably, PyrzA inhibited the hydroxylation of Pro402 and Pro564 on

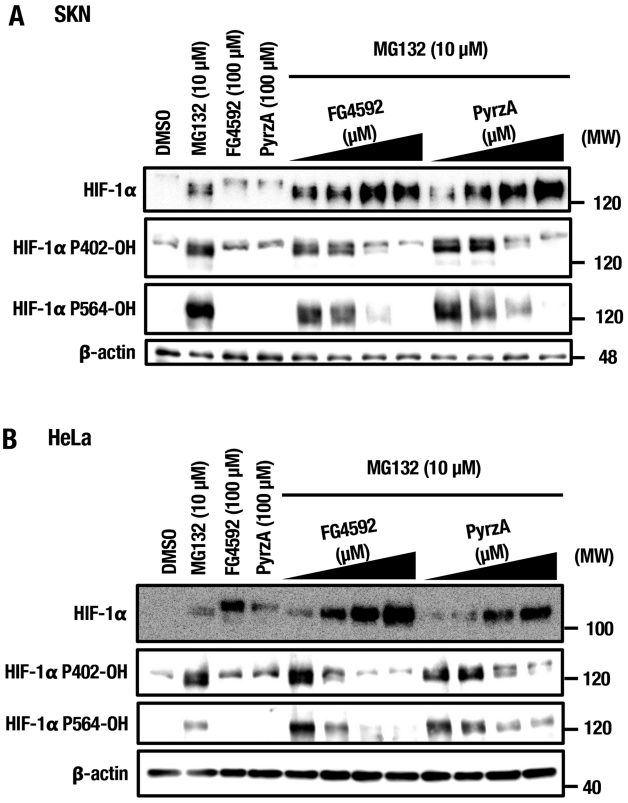

Figure 4. PyrzA inhibits HIF-1α prolyl hydroxylation. (A, B) Immunoblot analyses of HIF-α with its hydroxylated Pro402 and 564 residues on SKN (A) or HeLa (B). Cells were treated with various concentrations (1.0, 5.0, 25, or 100 μM) of PyrzA and FG4592 in the presence of proteasome inhibitor MG132 (10 μM) for 24 h. Simultaneously, cells were independently treated with PyrzA (100 μM), FG4592 (100 μM), or MG132 (10 μM) for 24 h. Equal loading was assessed by probing the blots with antibody against β-actin.

https://doi.org/10.1021/acsptsci.2c00002
ACS Pharmacol. Transl. Sci. 2022, 5, 362–372

HIF-1α when compared with FG4592 activity. Furthermore, PyrzA inhibited both Pro402 and Pro564 in HIF-1α hydroxylation. In future studies, we will make other PyrzA derivatives that can inhibit Pro402 and Pro564 on HIF-1α independently. We conclude that PyrzA stabilizes HIF-α by inhibiting PHDs as PyrzA decreases the hydroxylation of Pro402 or Pro564 on HIF-1α and FG4592.

PyrzA Upregulates HIF Target Genes. We showed that PyrzA could stabilize the HIF-α protein. To investigate HIF-α transcriptional activity, we measured the mRNA expression profiles of HIF target genes. To do this, we selected the carbonic anhydrase 9 (*CA9*), *PHD3*, and erythropoietin (*EPO*) genes. Hep3B cells (5.0×10^5 cells/well) were seeded into 3 cm dishes and preincubated for 16 h. After preincubation, the cells were challenged with PyrzA or FG4592 (10, 30, and 100 μM) for 24 h and the negative control vehicle, DMSO. PyrzA induced all selected genes and FG4592 at 100 μM (Figure 5A–C). The expression of the HIF target genes after treatment with PyrzA responded significantly from 30 to 100 μM.

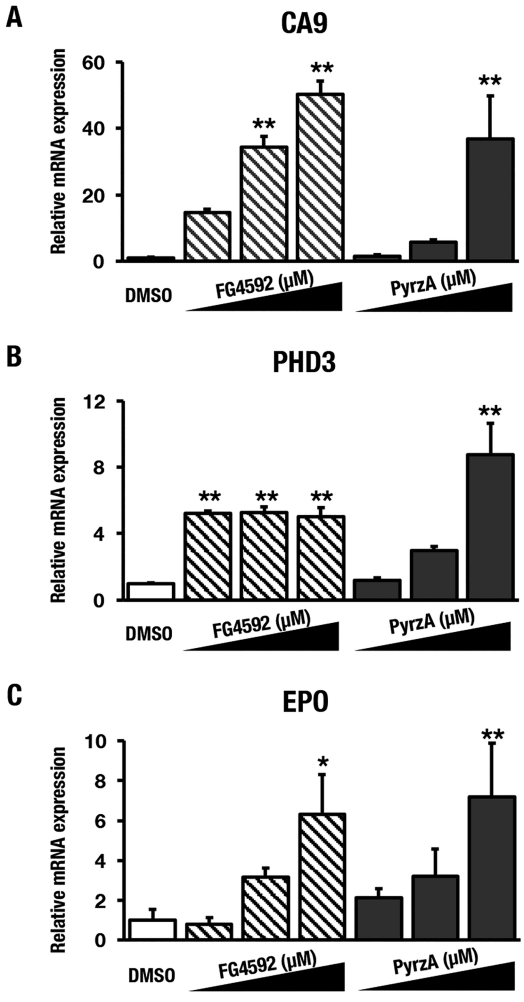

Figure 5. Effect of PyrzA on HIF-α target gene regulation. (A-C) The expression levels of carbonic anhydrase 9 (*CA9*), *PHD3*, and erythropoietin (*EPO*) were measured using RT-qPCR after treatment with FG4592 or PyrzA (10, 30, and 100 μM) for 24 h and Hep3B. Experiments were performed in triplicates. Each data is mean ± SEM (n = 3) and based on the value from 1% DMSO-treated cells set as 1. *P < 0.05, **P < 0.01 compared with 1% DMSO (one-way ANOVA with Dunnett test). All data are expressed as mean ± SEM.

Therefore, PyrzA is able to stabilize the HIF-α protein and stimulate the HIF signaling cascade.

PyrzA Upregulates HIF-α Expression in Mice. To examine whether PyrzA promoted HIF signaling in wild-type C57BL6 mice, we intraperitoneally administered 6-week-old female mice with PyrzA (50 mg/kg) or DMSO. Six hours after the PyrzA administration, we harvested blood and tissues from the treated mice for further examination. Plasma EPO protein is the primary inducer of erythropoiesis; hence, we measured the level of EPO using ELISA. We observed minute alterations in the levels of EPO in the PyrzA-treated group. However, the change was not statistically significant compared to the control group (Figure 6A). Moreover, we observed that the mRNA

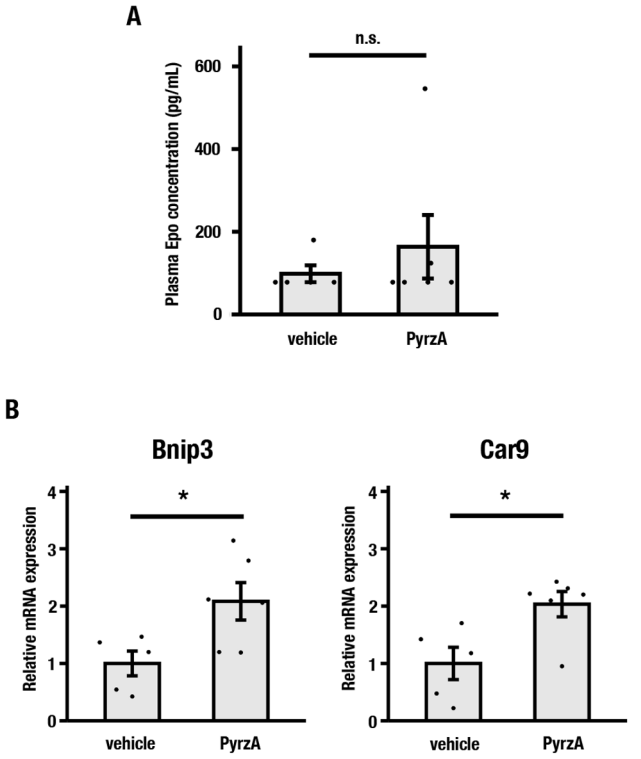

Figure 6. PyrzA activates HIF-α in mice. (A) Erythropoietin levels in PyrzA (50 mg/kg, i.p.)-treated mice plasma (n = 6) were normalized to vehicle control (n = 5). (B) The expression of BCL2/adenovirus E1B interacting protein 3 (*Bnip3*) and carbonic anhydrase 9 (*Car9*) was measured using RT-qPCR 6 h after PyrzA (50 mg/kg) or vehicle injection in the kidney. *P < 0.05 compared with vehicle (two-tailed, unpaired Student's t test). All data are expressed as mean ± SEM.

levels of the principal target genes of HIF-α, including BCL2/adenovirus E1B interacting protein 3 (*Bnip3*), and carbonic anhydrase 9 (*Car9*), were significantly upregulated in the kidneys of PyrzA-treated mice (Figure 6B). In conclusion, our initial hit, the potential HIF-α inducer PyrzA, effectively drives the HIF-α pathway, even *in vivo*. In future studies, we will optimize the bioavailability of PyrzA *in vivo* after the chemical modification of PyrzA.

Docking Simulation Using PyrzA with PHD2. We showed that PyrzA could inhibit hydroxylation on HIF-α prolyl residues (Figure 4). To predict the binding sites of PHD and PyrzA, we performed a docking simulation (Figure 7). We selected the human PHD2:Mn^{2+}:*N*-oxalylglycine:HIF-α substrate complex (PDB ID: 3hqr[48]) as a template structure using the Molegro Virtual Docker 7.0.0 (Figure S3B-D).[81] The

https://doi.org/10.1021/acsptsci.2c00002
ACS Pharmacol. Transl. Sci. 2022, 5, 362–372

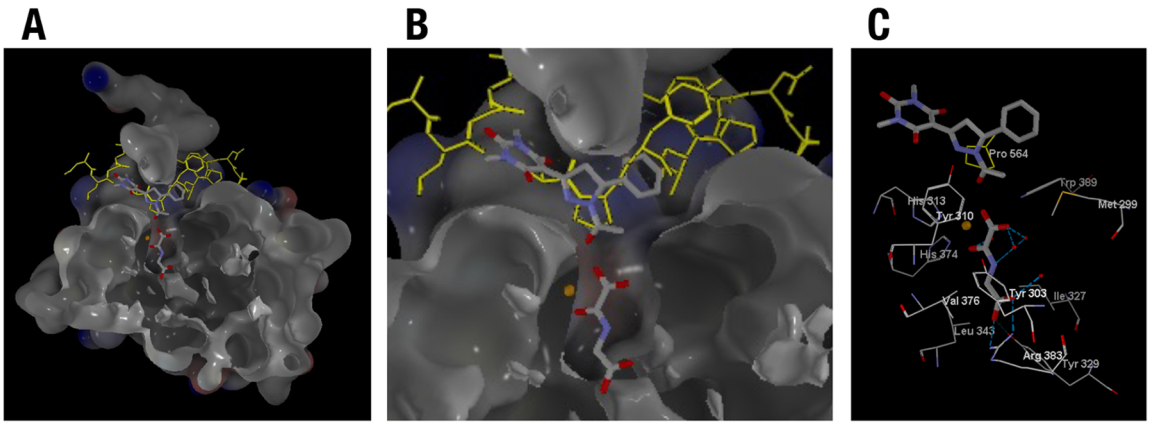

Figure 7. Predicted binding model of PHD2 (PDB ID: 3hqr) within PyrzA. HIF-1α CODD peptide (amino acids number 556−574) (yellow) bound to PHD2; blue corresponds to positive charge and red to negative charge residues. Mn^{2+} (orange) and *N*-oxalylglycine were substitutes for Fe^{2+} and 2-OG, respectively. PyrzA and *N*-oxalylglycine were drawn with carbon in white, oxygen in red, and nitrogen in blue. (A) Overall view. (B) Enlarged view of the area around the Pro564 (CODD). (C) Enlarged view of the catalytic center of PHD2 showing Mn^{2+}, 2-OG, (*S*)-PyrzA, Pro564, and the specified residues of PHD2.

coordinates of the five-membered ring structure of PyrzA were found to overlap the coordinates of Pro564 in HIF-1α CODD. Additionally, both of the racemic PyrzA, including (*S*)- or (*R*)-PyrzA, could bind to the PHD protein. Their docking (MolDoc) scores were −99.6763 and −89.3412 (kcal/mol), respectively (Figure 7 and Figure S3A, E, and F). Namely, PyrzA had the potential to interrupt the PHD2 and HIF-1α CODD binding. To the best of our knowledge, PHD inhibitors with HIF-1α CODD analogs have not been reported, and this may be the first study to do so. If the binding site of an inhibitor does not have a 2-OG vacancy, it may potentially have increased selectivity for enzymes with 2-OG as a cofactor over inhibitors of 2-OG analogs. The docking results indicate that PyrzA has that potential.

Experimental Measurement of the Partition Coefficient of PyrzA. We evaluated the LogP (partition coefficient in octanol/water) value experimentally to investigate the pharmacokinetics of PyrzA. The LogP value of PyrzA was 1.10 ± 0.09 and showed low lipophilicity. In the future, this pharmacological feature will be improved by synthesizing more efficient derivatives of this compound.

CONCLUSIONS

In this study, we reported a novel HIF activator, PyrzA, which does not harbor a 2-OG scaffold. Compared with the synthesis processes of known PHD inhibitors, including FG4592, PyrzA can be generated in three reasonable steps, which reduces the synthesis time and cost. PyrzA not only triggers the HIF signaling cascade, but also has markedly low cytotoxicity in mice. The efficacy of PyrzA as an activator of HIF is comparable to that of the known PHD inhibitor DMOG. PyrzA stabilizes the HIF protein in three types of cells and accumulates both the HIF-α isoforms (HIF-1α and HIF-2α). Most importantly, PyrzA is capable of upregulating HIF target genes including *EPO*. When the proteasomal degradation was inhibited by MG132 to prevent the degradation of hydroxylated HIF-1α, PyrzA remarkably suppressed the hydroxylated HIF-1α at both prolines. These findings suggest that PyrzA effectively inhibits PHDs. Although our current PyrzA biomolecule has the potential to promote the expression of several HIF target genes *in vivo*, the only limitation is that most PyrzA molecules are likely to be excreted through urine due to their low LogP value. Therefore, future research should primarily focus on optimizing the current PyrzA molecule to improve its bioavailability.

EXPERIMENTAL SECTION

Reagents. Dimethyl sulfoxide (DMSO) was purchased from Fujifilm Wako (Osaka, Japan). MG132 was obtained from Peptide Institution (Osaka, Japan). FG4592 was purchased from Cayman Chemical Company (Ann Arbor, MI, USA). DMOG was purchased from Merck (Darmstadt, Germany). All compounds used in this study were >95% pure, achieved by HPLC.

Chemical Synthesis of PyrzA. All starting materials, except (*E*)-1,3-dimethyl-5-(3-phenylacryloyl)barbituric acid, were obtained from commercial suppliers and used without additional purification. ^{1}H and ^{13}C NMR spectra were recorded using a NMR 400 MHz system (Agilent, Santa Clara, CA, USA). The chemical shift (δ) was assigned relative to $SiMe_4$ as an internal control at δ 0 ppm. High-resolution mass spectra were obtained using an Agilent G6224AA TOF-MS system.

(*E*)-1,3-Dimethyl-5-(3-phenylacryloyl)barbituric acid (**1**) was synthesized as described in the literature.[79]

*Synthesis of 1,3-Dimethyl-5-(5-phenylpyrazolidin-3-ylidene)barbituric Acid (**2**).* Under a nitrogen atmosphere, (*E*)-1,3-dimethyl-5-(3-phenylacryloyl)barbituric acid (**1**) (1 mmol), hydrazine monohydrate (2 mmol), and ethanol (30 mL) were placed in a 50 mL two-necked flask. The mixture was stirred under reflux for 1 h. After the reaction, a white precipitate was formed. After the precipitate was filtered, washed with ethanol, and dried, **2** was obtained in 84% yield. 1,3-dimethyl-5-(5-phenylpyrazolidin-3-ylidene)barbituric acid (**2**): white solid; ^{1}H NMR (400 MHz, $CDCl_3$) δ 3.28 (s, 3H), 3.31 (s, 3H), 3.74 (dd, J = 7.7, 18.9 Hz, 1H), 4.10 (dd, J = 9.2, 18.9 Hz, 1H), 4.80−4.88 (dd, J = 7.7, 9.2 Hz, 1H), 5.20 (d, J = 7.4 Hz, 1H), 7.29−7.40 (m, 5H), 12.02 (s, 1H); ^{13}C NMR (100 MHz, $CDCl_3$) δ 27.6, 27.7, 42.9, 59.5, 86.2, 126.2, 128.4, 129.0, 139.2, 151.8, 162.2, 164.9, 165.8. HRMS (TOF) calculated for $C_{15}H_{17}N_4O_3$ $[M + H]^+$: 301.1301; found: 301.1302.

*Synthesis of 5-(1-Acetyl-5-phenylpyrazolidin-3-ylidene)-1,3-dimethylbarbituric Acid (**3**).* Under a nitrogen atmos-

https://doi.org/10.1021/acsptsci.2c00002
ACS Pharmacol. Transl. Sci. 2022, 5, 362−372

phere, **2** (0.5 mmol), acetic acid (0.5 mL), and acetic anhydride (0.5 mL) were placed in a 25 mL two-necked flask. The mixture was stirred at 125 °C (bath temperature) for 2 h. After the reaction, the mixture was concentrated and dried under a vacuum. Purification was performed by recycling preparative HPLC using GPC columns with $CHCl_3$ as the eluent. After purification, compound **3** was obtained in 74% yield. 5-(1-acetyl-5-phenylpyrazolidin-3-ylidene)-1,3-dimethyl-barbituric acid (**3**): white solid; melting point was 273−274 °C. ^{1}H NMR (400 MHz, $CDCl_3$) δ 1.94 (s, 3H), 3.27 (s, 3H), 3.37 (s, 3H), 3.99 (dd, J = 2.5, 19.5 Hz, 1H), 4.30 (dd, J = 10.9, 19.5 Hz, 1H), 5.40 (d, J = 8.2 Hz, 1H), 7.23−7.28 (m, 2H), 7.31−7.47 (m, 3H), 13.19 (br, 1H); ^{13}C NMR (100 MHz, $CDCl_3$) δ 20.6, 27.7, 45.1, 58.6, 86.3, 125.0, 129.0, 129.7, 139.3, 151.6, 157.7, 162.1, 163.6, 164.3. HRMS (TOF) calculated for $C_{17}H_{19}N_4O_4$ $[M + H]^+$: 343.1406; found: 343.1437. Compound **3** was racemic; therefore, we used it as a racemic in the subsequent experiments.

Cell Culture. The human neuroblastoma cell line SKN and the human hepatocellular carcinoma cell line Hep3B were obtained from the American Type Culture Collection (ATCC; Manassas, VA, USA). The HeLa human cervical epithelioid carcinoma cell line was obtained from the RIKEN Bio Resource Center (Tsukuba, Ibaraki, Japan). SKN was cultured in RPMI1640 (Fujifilm Wako) then supplemented with 5% fetal bovine serum (EQUITEC-BIO, Kerrville, TX, USA) and 1% penicillin-streptomycin (Nacalai Tesque, Kyoto, Japan). HeLa and Hep3B cells were cultured in high-glucose DMEM (Fujifilm Wako). All cell lines were cultured in a humidified atmosphere containing 5% CO_2 at 37 °C.

High-Throughput Screening Using the SKN:HRE-NLuc Cell Line. SKN:HRE-NLuc cells, stable transformants of SKN with a reporter vector possessing secretion-type NLuc, were developed as previously described.[72] The SKN:HRE-NLuc cells (7.0×10^3 cells/well) were then seeded into a 384-well plate and incubated for 16 h. After incubation, the medium was replaced with new medium individually containing the core 9600 chemical library of the HTS compounds (20 μM final concentration with 1% DMSO) supplied by the Drug Development Initiative (DDI), The University of Tokyo, and treated for 24 h. The NLuc activity was measured with a Nano-Glo Luciferase Assay System (Promega, Madison, WI, USA) by SpectraMax Paradigm (Molecular Devices, Sunnyvale, CA, USA). To ensure the HTS accuracy, S/N, S/B, and Z'-factor were calculated using 1% DMSO as a negative control and 100 μM $CoCl_2$ as a 100% positive control.

Evaluation of HIF Activity and Cellular Viability. SKN:HRE-NLuc cells (7.0×10^3 cells/well) were seeded into a 384-well plate and incubated for 16 h. The medium was replaced with fresh medium containing the target compounds, PyrzA or FG4592, sequentially diluted from 100 μM to 98 nM. The cells were stimulated for 24 h. After incubation, the luciferase activity was measured using the Nano-Glo Luciferase Assay System by SpectraMax i3x (Molecular Devices). HIF activity was calculated as the intensity of luciferase activity based on the vehicle treatments (1% DMSO). To analyze cellular viability, the medium of chemically stimulated SKN:HRE-NLuc was replaced with new medium containing 1/10 (v/v) of CCK-8 assay reagents (Cell Counting Kit-8, Dojindo, Kumamoto, Japan) and incubated for 1 h. After incubation, the OD_{450} of CCK-8 reagents was measured using the SpectraMax i3x. Cell viability was presented as a percentage based on the cells stimulated with 1% DMSO and used as a positive control.

Immunoblot Assay. The cells were solubilized with SDS sample buffer (0.25 M Tris-HCl, pH 6.8, 20% [w/v] DTT, 8% [w/v] SDS, 20% [w/v] sucrose, 0.008% [w/v] bromophenol blue) and boiled at 90 °C for 10 min. The samples were subjected to SDS-PAGE electrophoresis and transferred to polyvinylidene fluoride membranes (Fujifilm Wako). The blots were incubated with primary antibodies against HIF-1α (Abnova, Taipei, Taiwan), Anti-HIF-1-alpha, hydroxyproline (Pro402) (Merck), Hydroxy-HIF-1α (Pro564) (Cell Signal Technology, Danvers, MA, USA), HIF-2α (Cell Signal Technology), or β-actin (Fujifilm Wako), and subsequently treated with immunogen-matched horseradish peroxidase-conjugated secondary antibodies. The proteins were visualized with ImmunoStar LD (Fujifilm Wako) using Lumino Graph I (ATTO, Tokyo, Japan).

RNA Isolation and Quantitative PCR. Total RNA from the cells was prepared using the Blood/Cultured Cell Total RNA Mini Kit (FAVORGEN, PingTung, Taiwan) following the manufacturer's instructions. Total RNA from the mouse liver was extracted using Sepasol RNA I Super G (Nacalai Tesque) according to the manufacturer's instructions. The total RNA was reverse transcribed to cDNA using the Transcriptor Universal cDNA Master (Roche, Basel, Switzerland). The resulting cDNA was used as a template for quantitative PCR (qPCR) using the KAPA SYBR FAST qPCR Master Mix (2×) Kit (Roche) with a LightCycler 96 system (Roche) and Mx3005P qPCR system (Agilent). β-actin expression levels were used as internal controls. The primer sequences used were as follows: human carbonic anhydrase 9 (CA9): (forward) 5′-CCTTTGCCAGAGTTGACGAG-3′ and (reverse) 5′-GACAGCAACTGCTCATAGGC-3′; human PHD3: (forward) 5′-CACGAAGTGCAGCCCTCT-TA-3′ and (reverse) 5′-TTGGCTTCTGCCCTTTCTTCA-3′; human erythropoietin (EPO): (forward) 5′-TCATCTGT-GACAGCCGAGTC -3′ and (reverse) 5′- CAAGCTG-CAGTGTTCAGCAC-3′; human β-actin: (forward) 5′-CCTCGCCTTTGCCGATCC -3′ and (reverse) 5′-CATGCCGGAGCCGTTGT-3′; mouse BCL2/adenovirus E1B interacting protein 3 (*Bnip3*): (forward) 5′-GTTACC-CACGAACCCCACTTT-3′ and (reverse) 5′-GTGGACAG-CAAGGCGAGAAT-3′; mouse carbonic anhydrase 9 (*Car9*): (forward) 5′-TGCTCCAAGTGTCTGCTCAG-3′ and (reverse) 5′-CAGGTGCATCCTCTTCACTGG-3′; and mouse 18S rRNA (forward): 5′-GTAACCCGTTGAACCCCATT-3′ and (reverse) 5′-CCATCCAATCGGTAGTAGC-3′.

Animals. All procedures for the mouse experiments were approved by the Animal Care Committee of Saga University and conformed with the Guide for the Care and Use of Laboratory Animals issued by the National Institute of Health. Six-week-old female C57B6 mice were housed in environments with a 12 h light/12 h dark cycle and constant temperature. PyrzA or corn oil (negative control) was administrated subcutaneously at 50 mg/kg body weight. Six hours after injection, blood and tissues were harvested from all mice.

Erythropoietin ELISA. Whole blood from the mice treated with PyrzA or the vehicle control was collected in a 1.5 mL tube containing heparin. Samples were spun at 5000 rpm for 5 min at 4 °C. The concentration of mice plasma was measured using an enzyme-linked immunosorbent assay (ELISA). The erythropoietin analysis was performed using the mouse erythropoietin ELISA kit (Proteintech, Rosemont, IL, USA)

https://doi.org/10.1021/acsptsci.2c00002
ACS Pharmacol. Transl. Sci. 2022, 5, 362−372

following the manufacturer's instructions. The detection and quantification of plasma EPO were performed using SpectraMax i3x with SoftMax Pro 7 (Molecular Devices). The detection limits of the samples were calculated as half of the detection limit.

Docking Simulation. To calculate the docking simulation between PHD2 and PyrzA, we used the Molegro Virtual Docker 7.0.0. We obtained the crystal structure data for PHD2 (PDB ID: 3hqr[48]) from the Protein Data Bank. The docking simulations were performed using the Molegro Virtual Docker 7.0.0.[81] To select a favorable binding mode, we used the MolDock score. The number of trial runs for calculations was 20. The chemical structures of the ligands were drawn using ChemBioDraw Ultra 20.0 and optimized by MM2 calculations in Chem3D Pro 20.0.

Experimental Measurement of the Partition Coefficient of PyrzA. A saturated octanol solution of PyrzA was prepared by adding 5.4 mg of PyrzA to 100 mL of octanol in a 200 mL beaker. The remaining PyrzA was removed by filtration, and 10 mL of the saturated PyrzA octanol solution and purified water were added to a separatory funnel, shaken, and allowed to stand to obtain an octanol layer and an aqueous layer, respectively. The absorbance of the octanol and aqueous layers was each measured at a maximum wavelength of 321 nm by a spectrophotometer (JASCO V-650, JASCO, Tokyo, Japan).

LogP = Log(absorption of octanol layer/absorption of water). This measurement was repeated three times and the average value was obtained.

Statistical Analysis. All data were expressed as mean ± standard error of the mean. All data were analyzed using one-way ANOVA or two-tailed, unpaired Student's *t* tests. For multiple comparisons, the Dunnett test was used.

■ ASSOCIATED CONTENT

Supporting Information

The Supporting Information is available free of charge at https://pubs.acs.org/doi/10.1021/acsptsci.2c00002.

^{1}H and ^{13}C NMR spectra for PyrzA, purity confirmation of the PyrzA, and docking simulation using PyrzA with PHD2 (PDF)

■ AUTHOR INFORMATION

Corresponding Author

Tadayuki Tsujita − *Laboratory of Biochemistry, Department of Applied Biochemistry and Food Science, Faculty of Agriculture, Saga University, Saga 840-8502, Japan; The United Graduate School of Agricultural Sciences, Kagoshima University, Kagoshima 890-0065, Japan;* orcid.org/0000-0002-7189-0376; Email: tada@cc.saga-u.ac.jp

Authors

Kento Sonoda − *Laboratory of Biochemistry, Department of Applied Biochemistry and Food Science, Faculty of Agriculture, Saga University, Saga 840-8502, Japan; Center for Education and Research in Agricultural Innovation, Faculty of Agriculture, Saga University, Saga 847-0021, Japan; The United Graduate School of Agricultural Sciences, Kagoshima University, Kagoshima 890-0065, Japan*

Sudarma Bogahawaththa − *Laboratory of Biochemistry, Department of Applied Biochemistry and Food Science, Faculty of Agriculture, Saga University, Saga 840-8502, Japan; Center for Education and Research in Agricultural Innovation, Faculty of Agriculture, Saga University, Saga 847-0021, Japan; The United Graduate School of Agricultural Sciences, Kagoshima University, Kagoshima 890-0065, Japan*

Akito Katayama − *Center for Education and Research in Agricultural Innovation, Faculty of Agriculture, Saga University, Saga 847-0021, Japan*

Saki Ujike − *Center for Education and Research in Agricultural Innovation, Faculty of Agriculture, Saga University, Saga 847-0021, Japan*

Sae Kuroki − *Center for Education and Research in Agricultural Innovation, Faculty of Agriculture, Saga University, Saga 847-0021, Japan*

Naho Kitagawa − *Laboratory of Biochemistry, Department of Applied Biochemistry and Food Science, Faculty of Agriculture, Saga University, Saga 840-8502, Japan*

Kohichi Hirotsuru − *Laboratory of Biochemistry, Department of Applied Biochemistry and Food Science, Faculty of Agriculture, Saga University, Saga 840-8502, Japan*

Norio Suzuki − *Division of Oxygen Biology, United Centers for Advanced Research and Translational Medicine, Tohoku University Graduate School of Medicine, Sendai, Miyagi 980-8575, Japan; Applied Oxygen Physiology Project, New Industry Creation Hatchery Center (NICHe), Tohoku University, Sendai, Miyagi 980-8575, Japan*

Toshio Miyata − *Department of Molecular Medicine and Therapy, Tohoku University Graduate School of Medicine, Sendai, Miyagi 980-8575, Japan*

Shin-ichi Kawaguchi − *Center for Education and Research in Agricultural Innovation, Faculty of Agriculture, Saga University, Saga 847-0021, Japan; The United Graduate School of Agricultural Sciences, Kagoshima University, Kagoshima 890-0065, Japan;* orcid.org/0000-0002-4140-9959

Complete contact information is available at: https://pubs.acs.org/10.1021/acsptsci.2c00002

Funding

This research was funded by the JSPS KAKENHI grants 17K19916 (T.T.), 19H04057 (T.T.), and 19K17746 (S.-i.K.) and the Basis for Supporting Innovative Drug Discovery and Life Science Research (BINDS) from AMED under the grant number JP17am0101095 (N.S., T.M., S.-i.K., and T.T.).

Notes

The authors declare the following competing financial interest(s): S-i.K. and T.T. are advisory members for Tetra Create Co., Ltd. All other authors declare no conflicts of interest.

Samples of the compounds are available from Tetra Create Co., Ltd.

■ ACKNOWLEDGMENTS

We acknowledge Dr. Nobuo Watanabe and for technical suggestions and valuable discussions. We also thank Sayaka Ito and Satomi Goto for technical assistance, the Biomedical Research Core of Tohoku University Graduate School of Medicine and Analytical Research Center for Experimental Sciences, and Saga University for technical support.

■ ABBREVIATIONS

PyrzA, 5-(1-acetyl-5-phenylpyrazolidin-3-ylidene)-1,3-dimethylbarbituric acid; HIF-α, hypoxia inducible factor-α; 2-OG, 2-oxoglutarate; PHDs, prolyl hydroxylase domain containing proteins; VEGF, vascular endothelial growth factor; EPO, erythropoietin; GLUT1, glucose transporter 1; PAS, PER-ARNT-SIM; bHLH, basic helix−loop−helix; HRE, hypoxia response element; ODDs, oxygen-dependent degradation domains; pVHL, von Hippel−Lindau protein; CKD, chronic kidney disease; HTS, high-throughput screening; SKN:HRE-NLuc, SK-N-BE(2)c cells that stably harbored a nanoluciferase reporter system construct; DDI, Drug Discovery Initiative, University of Tokyo; DMSO, dimethyl sulfoxide; CCK-8, Cell Counting Kit-8; CA9 or Car9, carbonic anhydrase 9; Bnip3, BCL2/adenovirus E1B interacting protein 3

■ REFERENCES

(1) Semenza, G. L. Oxygen Sensing, Homeostasis, and Disease. *N. Engl. J. Med.* **2011**, *365* (6), 537−547.

(2) Fraisl, P.; Aragonés, J.; Carmeliet, P. Inhibition of Oxygen Sensors as a Therapeutic Strategy for Ischaemic and Inflammatory Disease. *Nat. Rev. Drug Discovery* **2009**, *8* (2), 139−152.

(3) Venkatachalam, M. A.; Griffin, K. A.; Lan, R.; Geng, H.; Saikumar, P.; Bidani, A. K. Acute Kidney Injury: A Springboard for Progression in Chronic Kidney Disease. *Am. J. Physiol. - Ren. Physiol.* **2010**, *298* (5), 1078−1094.

(4) Matsumoto, M.; Makino, Y.; Tanaka, T.; Tanaka, H.; Ishizaka, N.; Noiri, E.; Fujita, T.; Nangaku, M. Induction of Renoprotective Gene Expression by Cobalt Ameliorates Ischemic Injury of the Kidney in Rats. *J. Am. Soc. Nephrol.* **2003**, *14* (7), 1825−1832.

(5) Macheda, M. L.; Rogers, S.; Best, J. D. Molecular and Cellular Regulation of Glucose Transporter (GLUT) Proteins in Cancer. *J. Cell. Physiol.* **2005**, *202* (3), 654−662.

(6) Fraisl, P.; Mazzone, M.; Schmidt, T.; Carmeliet, P. Regulation of Angiogenesis by Oxygen and Metabolism. *Dev. Cell* **2009**, *16* (2), 167−179.

(7) Kamba, T.; McDonald, D. M. Mechanisms of Adverse Effects of Anti-VEGF Therapy for Cancer. *Br. J. Cancer* **2007**, *96* (12), 1788−1795.

(8) Rankin, E. B.; Rha, J.; Unger, T. L.; Wu, C. H.; Shutt, H. P.; Johnson, R. S.; Simon, M. C.; Keith, B.; Haase, V. H. Hypoxia-Inducible Factor-2 Regulates Vascular Tumorigenesis in Mice. *Oncogene* **2008**, *27* (40), 5354−5358.

(9) Kaelin, W. G.; Ratcliffe, P. J. Oxygen Sensing by Metazoans: The Central Role of the HIF Hydroxylase Pathway. *Mol. Cell* **2008**, *30* (4), 393−402.

(10) Majmundar, A. J.; Wong, W. J.; Simon, M. C. Hypoxia-Inducible Factors and the Response to Hypoxic Stress. *Mol. Cell* **2010**, *40* (2), 294−309.

(11) Koury, M. J.; Haase, V. H. Anaemia in Kidney Disease: Harnessing Hypoxia Responses for Therapy. *Nat. Rev. Nephrol.* **2015**, *11* (7), 394−410.

(12) Chan, M. C.; Holt-Martyn, J. P.; Schofield, C. J.; Ratcliffe, P. J. Pharmacological Targeting of the HIF Hydroxylases - A New Field in Medicine Development. *Mol. Aspects Med.* **2016**, *47*−*48*, 54−75.

(13) Yeh, T. L.; Leissing, T. M.; Abboud, M. I.; Thinnes, C. C.; Atasoylu, O.; Holt-Martyn, J. P.; Zhang, D.; Tumber, A.; Lippl, K.; Lohans, C. T.; Leung, I. K. H.; Morcrette, H.; Clifton, I. J.; Claridge, T. D. W.; Kawamura, A.; Flashman, E.; Lu, X.; Ratcliffe, P. J.; Chowdhury, R.; Pugh, C. W.; Schofield, C. J. Molecular and Cellular Mechanisms of HIF Prolyl Hydroxylase Inhibitors in Clinical Trials. *Chem. Sci.* **2017**, *8* (11), 7651−7668.

(14) Semenza, G. L.; Wang, G. L. A Nuclear Factor Induced by Hypoxia via de Novo Protein Synthesis Binds to the Human Erythropoietin Gene Enhancer at a Site Required for Transcriptional Activation. *Mol. Cell. Biol.* **1992**, *12* (12), 5447−5454.

(15) Wang, G. L.; Semenza, G. L. General Involvement of Hypoxia-Inducible Factor 1 in Transcriptional Response to Hypoxia. *Proc. Natl. Acad. Sci. U. S. A.* **1993**, *90* (9), 4304−4308.

(16) Weidemann, A.; Johnson, R. S. Biology of HIF-1α. *Cell Death Differ.* **2008**, *15* (4), 621−627.

(17) Wang, G. L.; Jiang, B. H.; Rue, E. A.; Semenza, G. L. Hypoxia-Inducible Factor 1 Is a Basic-Helix-Loop-Helix-PAS Heterodimer Regulated by Cellular O_2 Tension. *Proc. Natl. Acad. Sci. U. S. A.* **1995**, *92* (12), 5510−5514.

(18) Wang, G. L.; Semenza, G. L. Purification and Characterization of Hypoxia-Inducible Factor. *J. Biol. Chem.* **1995**, *270* (3), 1230−1237.

(19) Kimura, H.; Weisz, A.; Ogura, T.; Hitomi, Y.; Kurashima, Y.; Hashimoto, K.; D'Acquisto, F.; Makuuchi, M.; Esumi, H. Identification of Hypoxia-Inducible Factor 1 Ancillary Sequence and Its Function in Vascular Endothelial Growth Factor Gene Induction by Hypoxia and Nitric Oxide. *J. Biol. Chem.* **2001**, *276* (3), 2292−2298.

(20) Bruick, R. K. Oxygen Sensing in the Hypoxic Response Pathway: Regulation of the Hypoxia-Inducible Transcription Factor. *Genes Dev.* **2003**, *17* (21), 2614−2623.

(21) Berra, E.; Benizri, E.; Ginouvès, A.; Volmat, V.; Roux, D.; Pouysségur, J. HIF Prolyl-Hydroxylase 2 Is the Key Oxygen Sensor Setting Low Steady-State Levels of HIF-1α in Normoxia. *EMBO J.* **2003**, *22* (16), 4082−4090.

(22) Masson, N.; Willam, C.; Maxwell, P. H.; Pugh, C. W.; Ratcliffe, P. J. Independent Function of Two Destruction Domains in Hypoxia-Inducible Factor-α Chains Activated by Prolyl Hydroxylation. *EMBO J.* **2001**, *20* (18), 5197−5206.

(23) Maxwell, P. H.; Wiesener, M. S.; Chang, G. W.; Clifford, S. C.; Vaux, E. C.; Cockman, M. E.; Wykoff, C. C.; Pugh, C. W.; Maher, E. R.; Ratcliffe, P. J. The Tumour Suppressor Protein VHL Targets Hypoxia-Inducible Factors for Oxygen-Dependent Proteolysis. *Nature* **1999**, *399* (6733), 271−275.

(24) Jaakkola, P.; Mole, D. R.; Tian, Y. M.; Wilson, M. I.; Gielbert, J.; Gaskell, S. J.; Kriegsheim, A. V.; Hebestreit, H. F.; Mukherji, M.; Schofield, C. J.; Maxwell, P. H.; Pugh, C. W.; Ratcliffe, P. J. Targeting of HIF-α to the von Hippel-Lindau Ubiquitylation Complex by O_2-Regulated Prolyl Hydroxylation. *Science* **2001**, *292* (5516), 468−472.

(25) Ivan, M.; Kondo, K.; Yang, H.; Kim, W.; Valiando, J.; Ohh, M.; Salic, A.; Asara, J. M.; Lane, W. S.; Kaelin, W. G. HIFα Targeted for VHL-Mediated Destruction by Proline Hydroxylation: Implications for O_2 Sensing. *Science* **2001**, *292* (5516), 464−468.

(26) Min, J. H.; Yang, H.; Ivan, M.; Gertler, F.; Kaelin, W. G.; Pavletich, N. P. Structure of an HIF-1α-pVHL Complex: Hydroxyproline Recognition in Signaling. *Science* **2002**, *296* (5574), 1886−1889.

(27) Fong, G. H.; Takeda, K. Role and Regulation of Prolyl Hydroxylase Domain Proteins. *Cell Death Differ.* **2008**, *15* (4), 635−641.

(28) Minamishima, Y. A.; Moslehi, J.; Bardeesy, N.; Cullen, D.; Bronson, R. T.; Kaelin, W. G. Somatic Inactivation of the PHD2 Prolyl Hydroxylase Causes Polycythemia and Congestive Heart Failure. *Blood* **2008**, *111* (6), 3236−3244.

(29) Gordan, J. D.; Lal, P.; Dondeti, V. R.; Letrero, R.; Parekh, K. N.; Oquendo, C. E.; Greenberg, R. A.; Flaherty, K. T.; Rathmell, W. K.; Keith, B.; Simon, M. C.; Nathanson, K. L. HIF-α Effects on c-Myc Distinguish Two Subtypes of Sporadic VHL-Deficient Clear Cell Renal Carcinoma. *Cancer Cell* **2008**, *14* (6), 435−446.

(30) Takeda, K.; Ho, V. C.; Takeda, H.; Duan, L. J.; Nagy, A.; Fong, G. H. Placental but Not Heart Defects Are Associated with Elevated Hypoxia-Inducible Factor α Levels in Mice Lacking Prolyl Hydroxylase Domain Protein 2. *Mol. Cell. Biol.* **2006**, *26* (22), 8336−8346.

(31) Tojo, Y.; Sekine, H.; Hirano, I.; Pan, X.; Souma, T.; Tsujita, T.; Kawaguchi, S-i.; Takeda, N.; Takeda, K.; Fong, G. H.; Dan, T.; Ichinose, M.; Miyata, T.; Yamamoto, M.; Suzuki, N. Hypoxia Signaling Cascade for Erythropoietin Production in Hepatocytes. *Mol. Cell. Biol.* **2015**, *35* (15), 2658−2672.

(32) Souma, T.; Nezu, M.; Nakano, D.; Yamazaki, S.; Hirano, I.; Sekine, H.; Dan, T.; Takeda, K.; Fong, G. H.; Nishiyama, A.; Ito, S.;

https://doi.org/10.1021/acsptsci.2c00002
ACS Pharmacol. Transl. Sci. 2022, 5, 362−372

Miyata, T.; Yamamoto, M.; Suzuki, N. Erythropoietin Synthesis in Renal Myofibroblasts Is Restored by Activation of Hypoxia Signaling. *J. Am. Soc. Nephrol.* **2016**, *27* (2), 428−438.
(33) Appelhoff, R. J.; Tian, Y. M.; Raval, R. R.; Turley, H.; Harris, A. L.; Pugh, C. W.; Ratcliffe, P. J.; Gleadle, J. M. Differential Function of the Prolyl Hydroxylases PHD1, PHD2, and PHD3 in the Regulation of Hypoxia-Inducible Factor. *J. Biol. Chem.* **2004**, *279* (37), 38458−38465.
(34) Jokilehto, T.; Jaakkola, P. M. The Role of HIF Prolyl Hydroxylases in Tumour Growth. *J. Cell. Mol. Med.* **2010**, *14* (4), 758−770.
(35) Tian, H.; McKnight, S. L.; Russell, D. W. Endothelial PAS Domain Protein 1 (EPAS1), a Transcription Factor Selectively Expressed in Endothelial Cells. *Genes Dev.* **1997**, *11* (1), 72−82.
(36) Ema, M.; Taya, S.; Yokotani, N.; Sogawa, K.; Matsuda, Y.; Fujii-Kuriyama, Y. A Novel BHLH-PAS Factor with Close Sequence Similarity to Hypoxia-Inducible Factor 1α Regulates the VEGF Expression and Is Potentially Involved in Lung and Vascular Development. *Proc. Natl. Acad. Sci. U. S. A.* **1997**, *94* (9), 4273−4278.
(37) Flamme, I.; Fröhlich, T.; von Reutern, M.; Kappel, A.; Damert, A.; Risau, W. HRF, a Putative Basic Helix-Loop-Helix-PAS-Domain Transcription Factor Is Closely Related to Hypoxia-Inducible Factor-1α and Developmentally Expressed in Blood Vessels. *Mech. Dev.* **1997**, *63* (1), 51−60.
(38) Holmquist-Mengelbier, L.; Fredlund, E.; Löfstedt, T.; Noguera, R.; Navarro, S.; Nilsson, H.; Pietras, A.; Vallon-Christersson, J.; Borg, Å.; Gradin, K.; Poellinger, L.; Påhlman, S. Recruitment of HIF-1α and HIF-2α to Common Target Genes Is Differentially Regulated in Neuroblastoma: HIF-2α Promotes an Aggressive Phenotype. *Cancer Cell* **2006**, *10* (5), 413−423.
(39) Koh, M. Y.; Lemos, R.; Liu, X.; Powis, G. The Hypoxia-Associated Factor Switches Cells from HIF-1α- to HIF-2α-Dependent Signaling Promoting Stem Cell Characteristics, Aggressive Tumor Growth and Invasion. *Cancer Res.* **2011**, *71* (11), 4015−4027.
(40) Florczyk, U.; Czauderna, S.; Stachurska, A.; Tertil, M.; Nowak, W.; Kozakowska, M.; Poellinger, L.; Jozkowicz, A.; Loboda, A.; Dulak, J. Opposite Effects of HIF-1α and HIF-2α on the Regulation of IL-8 Expression in Endothelial Cells. *Free Radic. Biol. Med.* **2011**, *51* (10), 1882−1892.
(41) Hamidian, A.; von Stedingk, K.; Munksgaard Thorén, M.; Mohlin, S.; Påhlman, S. Differential Regulation of HIF-1α and HIF-2α in Neuroblastoma: Estrogen-Related Receptor Alpha (ERRα) Regulates HIF2A Transcription and Correlates to Poor Outcome. *Biochem. Biophys. Res. Commun.* **2015**, *461* (3), 560−567.
(42) Downes, N. L.; Laham-Karam, N.; Kaikkonen, M. U.; Ylä-Herttuala, S. Differential but Complementary HIF1α and HIF2α Transcriptional Regulation. *Mol. Ther.* **2018**, *26* (7), 1735−1745.
(43) Smythies, J. A.; Sun, M.; Masson, N.; Salama, R.; Simpson, P. D.; Murray, E.; Neumann, V.; Cockman, M. E.; Choudhry, H.; Ratcliffe, P. J.; Mole, D. R. Inherent DNA-binding Specificities of the HIF-1α and HIF-2α Transcription Factors in Chromatin. *EMBO Rep.* **2019**, *20* (1), e46401.
(44) Koshiji, M.; Kageyama, Y.; Pete, E. A.; Horikawa, I.; Barrett, J. C.; Huang, L. E. HIF-1α Induces Cell Cycle Arrest by Functionally Counteracting Myc. *EMBO J.* **2004**, *23* (9), 1949−1956.
(45) Koshiji, M.; To, K. K. W.; Hammer, S.; Kumamoto, K.; Harris, A. L.; Modrich, P.; Huang, L. E. HIF-1α Induces Genetic Instability by Transcriptionally Downregulating MutSα Expression. *Mol. Cell* **2005**, *17* (6), 793−803.
(46) Das, B.; Bayat-Mokhtari, R.; Tsui, M.; Lotfi, S.; Tsuchida, R.; Felsher, D. W.; Yeger, H. HIF-2α Suppresses p53 to Enhance the Stemness and Regenerative Potential of Human Embryonic Stem Cells. *Stem Cells* **2012**, *30* (8), 1685−1695.
(47) McDonough, M. A.; Li, V.; Flashman, E.; Chowdhury, R.; Mohr, C.; Liénard, B. M. R.; Zondlo, J.; Oldham, N. J.; Clifton, I. J.; Lewis, J.; McNeill, L. A.; Kurzeja, R. J. M.; Hewitson, K. S.; Yang, E.; Jordan, S.; Syed, R. S.; Schofield, C. J. Cellular Oxygen Sensing: Crystal Structure of Hypoxia-Inducible Factor Prolyl Hydroxylase (PHD2). *Proc. Natl. Acad. Sci. U. S. A.* **2006**, *103* (26), 9814−9819.
(48) Chowdhury, R.; McDonough, M. A.; Mecinović, J.; Loenarz, C.; Flashman, E.; Hewitson, K. S.; Domene, C.; Schofield, C. J. Structural Basis for Binding of Hypoxia-Inducible Factor to the Oxygen-Sensing Prolyl Hydroxylases. *Structure* **2009**, *17* (7), 981−989.
(49) Rabinowitz, M. H. Inhibition of Hypoxia-Inducible Factor Prolyl Hydroxylase Domain Oxygen Sensors: Tricking the Body into Mounting Orchestrated Survival and Repair Responses. *J. Med. Chem.* **2013**, *56* (23), 9369−9402.
(50) Rose, N. R.; McDonough, M. A.; King, O. N. F.; Kawamura, A.; Schofield, C. J. Inhibition of 2-Oxoglutarate Dependent Oxygenases. *Chem. Soc. Rev.* **2011**, *40* (8), 4364−4397.
(51) Miyata, T.; Suzuki, N.; van Ypersele de Strihou, C. Diabetic Nephropathy: Are There New and Potentially Promising Therapies Targeting Oxygen Biology? *Kidney Int.* **2013**, *84* (4), 693−702.
(52) Richard, M. K. Prolyl Hydroxylase Inhibitors and Methods of Use. U.S. Patent US2007/0299086, 2007.
(53) Ogoshi, Y.; Matsui, T.; Mitani, I.; Yokota, M.; Terashita, M.; Motoda, D.; Ueyama, K.; Hotta, T.; Ito, T.; Hase, Y.; Fukui, K.; Deai, K.; Yoshiuchi, H.; Ito, S.; Abe, H. Discovery of JTZ-951: A HIF Prolyl Hydroxylase Inhibitor for the Treatment of Renal Anemia. *ACS Med. Chem. Lett.* **2017**, *8* (12), 1320−1325.
(54) Duffy, K. J.; Fitch, D. M.; Jin, J.; Liu, R.; Shaw, A. N.; Wiggall, K. Prolyl Hydroxylase Inhibitors. PCT Int. Appl. WO2007/150011, 2007.
(55) Thevis, M.; Milosovich, S.; Licea-Perez, H.; Knecht, D.; Cavalier, T.; Schänzer, W. Mass Spectrometric Characterization of a Prolyl Hydroxylase Inhibitor GSK1278863, Its Bishydroxylated Metabolite, and Its Implementation into Routine Doping Controls. *Drug Test. Anal.* **2016**, *8* (8), 858−863.
(56) Beck, H.; Jeske, M.; Thede, K.; Stoll, F.; Flamme, I.; Akbaba, M.; Ergüden, J. K.; Karig, G.; Keldenich, J.; Oehme, F.; Militzer, H. C.; Hartung, I. V.; Thuss, U. Discovery of Molidustat (BAY 85−3934): A Small-Molecule Oral HIF-Prolyl Hydroxylase (HIF-PH) Inhibitor for the Treatment of Renal Anemia. *ChemMedChem.* **2018**, *13* (10), 988−1003.
(57) Desai, R. C.; Pandya, V.; Patel, P. R. Novel Quinolone Derivatives. PCT Int. Appl. WO2014/102818, 2014.
(58) Rosen, M. D.; Venkatesan, H.; Peltier, H. M.; Bembenek, S. D.; Kanelakis, K. C.; Zhao, L. X.; Leonard, B. E.; Hocutt, F. M.; Wu, X.; Palomino, H. L.; Brondstetter, T. I.; Haugh, P. V.; Cagnon, L.; Yan, W.; Liotta, L. A.; Young, A.; Mirzadegan, T.; Shankley, N. P.; Barrett, T. D.; Rabinowitz, M. H. Benzimidazole-2-Pyrazole HIF Prolyl 4-Hydroxylase Inhibitors as Oral Erythropoietin Secretagogues. *ACS Med. Chem. Lett.* **2010**, *1* (9), 526−529.
(59) Vachal, P.; Miao, S.; Pierce, J. M.; Guiadeen, D.; Colandrea, V. J.; Wyvratt, M. J.; Salowe, S. P.; Sonatore, L. M.; Milligan, J. A.; Hajdu, R.; Gollapudi, A.; Keohane, C. A.; Lingham, R. B.; Mandala, S. M.; DeMartino, J. A.; Tong, X.; Wolff, M.; Steinhuebel, D.; Kieczykowski, G. R.; Fleitz, F. J.; Chapman, K.; Athanasopoulos, J.; Adam, G.; Akyuz, C. D.; Jena, D. K.; Lusen, J. W.; Meng, J.; Stein, B. D.; Xia, L.; Sherer, E. C.; Hale, J. J. 1,3,8-Triazaspiro[4.5]Decane-2,4-Diones as Efficacious Pan-Inhibitors of Hypoxia-Inducible Factor Prolyl Hydroxylase 1−3 (HIF PHD1−3) for the Treatment of Anemia. *J. Med. Chem.* **2012**, *55* (7), 2945−2959.
(60) Hamada, M.; Takayama, T.; Shibata, T.; Hiratate, A.; Takahashi, M.; Yashiro, M.; Takayama, N.; Okumura-Kitajima, L.; Koretsune, H.; Kajiyama, H.; Naruse, T.; Kato, S.; Takano, H.; Kakinuma, H. Discovery of Novel 2-[(4-Hydroxy-6-Oxo-2,3-Dihydro-1H-Pyridine-5-Carbonyl)Amino]Acetic Acid Derivatives as HIF Prolyl Hydroxylase Inhibitors for Treatment of Renal Anemia. *Bioorg. Med. Chem. Lett.* **2018**, *28* (10), 1725−1730.
(61) Goi, T.; Nakajima, T.; Komatsu, Y.; Kawata, A.; Yamakoshi, S.; Okada, O.; Sugahara, M.; Umeda, A.; Takada, Y.; Murakami, J.; Ohashi, R.; Watanabe, T.; Fukase, K. Pyrazolo[4,3- d]Pyrimidine Derivatives as a Novel Hypoxia-Inducible Factor Prolyl Hydroxylase Domain Inhibitor for the Treatment of Anemia. *ACS Med. Chem. Lett.* **2020**, *11* (7), 1416−1420.

https://doi.org/10.1021/acsptsci.2c00002
ACS Pharmacol. Transl. Sci. 2022, 5, 362−372

(62) Dhillon, S. Roxadustat: First Global Approval. *Drugs* **2019**, *79* (5), 563−572.
(63) Arend, M. P.; Flippin, L. A.; Guenzler-pukall, V.; Ho, W. B.; Turtle, E. D.; Du, X. Nitrogen-Containing Heteroaryl Compounds and Their Use in Increasing Endogenous Erythropoietin. PCT Int. Appl. WO2004/108681, 2004.
(64) Loenarz, C.; Schofield, C. J. Physiological and Biochemical Aspects of Hydroxylations and Demethylations Catalyzed by Human 2-Oxoglutarate Oxygenases. *Trends Biochem. Sci.* **2011**, *36* (1), 7−18.
(65) Molle, I. V.; Thomann, A.; Buckley, D. L.; So, E. C.; Lang, S.; Crews, C. M.; Ciulli, A. Dissecting Fragment-Based Lead Discovery at the von Hippel-Lindau Protein: Hypoxia Inducible Factor 1α Protein-Protein Interface. *Chem. Biol.* **2012**, *19* (10), 1300−1312.
(66) Frost, J.; Galdeano, C.; Soares, P.; Gadd, M. S.; Grzes, K. M.; Ellis, L.; Epemolu, O.; Shimamura, S.; Bantscheff, M.; Grandi, P.; Read, K. D.; Cantrell, D. A.; Rocha, S.; Ciulli, A. Potent and Selective Chemical Probe of Hypoxic Signalling Downstream of HIF-α Hydroxylation via VHL Inhibition. *Nat. Commun.* **2016**, *7*, 1−12.
(67) Banerji, B.; Conejo-Garcia, A.; McNeill, L. A.; McDonough, M. A.; Buck, M. R. G.; Hewitson, K. S.; Oldham, N. J.; Schofield, C. J. The Inhibition of Factor Inhibiting Hypoxia-Inducible Factor (FIH) by β-Oxocarboxylic Acids. *Chem. Commun.* **2005**, *43*, 5438−5440.
(68) McDonough, M. A.; McNeill, L. A.; Tilliet, M.; Papamicaël, C. A.; Chen, Q. Y.; Banerji, B.; Hewitson, K. S.; Schofield, C. J. Selective Inhibition of Factor Inhibiting Hypoxia-Inducible Factor. *J. Am. Chem. Soc.* **2005**, *127* (21), 7680−7681.
(69) Conejo-Garcia, A.; McDonough, M. A.; Loenarz, C.; McNeill, L. A.; Hewitson, K. S.; Ge, W.; Liénard, B. M.; Schofield, C. J.; Clifton, I. J. Structural Basis for Binding of Cyclic 2-Oxoglutarate Analogues to Factor-Inhibiting Hypoxia-Inducible Factor. *Bioorg. Med. Chem. Lett.* **2010**, *20* (20), 6125−6128.
(70) Kawaguchi, S-i; Gonda, Y.; Yamamoto, T.; Sato, Y.; Shinohara, H.; Kobiki, Y.; Ichimura, A.; Dan, T.; Sonoda, M.; Miyata, T.; Ogawa, A.; Tsujita, T. Furan- and Thiophene-2-Carbonyl Amino Acid Derivatives Activate Hypoxia-Inducible Factor via Inhibition of Factor Inhibiting Hypoxia-Inducible Factor-1. *Molecules* **2018**, *23* (4), 885.
(71) Chan, M. C.; Ilott, N. E.; Schödel, J.; Sims, D.; Tumber, A.; Lippl, K.; Mole, D. R.; Pugh, C. W.; Ratcliffe, P. J.; Ponting, C. P.; Schofield, C. J. Tuning the Transcriptional Response to Hypoxia by Inhibiting Hypoxia-Inducible Factor (HIF) Prolyl and Asparaginyl Hydroxylases. *J. Biol. Chem.* **2016**, *291* (39), 20661−20673.
(72) Tsujita, T.; Kawaguchi, S-i. I.; Dan, T.; Baird, L.; Miyata, T.; Yamamoto, M. Hypoxia-Sensitive Reporter System for High-Throughput Screening. *Tohoku J. Exp. Med.* **2015**, *235* (2), 151−159.
(73) Kawaguchi, S.-i.; Tsujita, T. Novel nitrogen-containing cyclic compounds and their applications. Japan Patent JP2021/6904528, 2021.
(74) Majamaa, K.; Günzler, V.; Hanauske-Abel, H. M.; Myllylä, R.; Kivirikko, K. I. Partial Identity of the 2-Oxoglutarate and Ascorbate Binding Sites of Prolyl 4-Hydroxylase. *J. Biol. Chem.* **1986**, *261* (17), 7819−7823.
(75) Davis, C. K.; Jain, S. A.; Bae, O. N.; Majid, A.; Rajanikant, G. K. Hypoxia Mimetic Agents for Ischemic Stroke. *Front. Cell Dev. Biol.* **2019**, *6*, 175.
(76) Smirnova, N. A.; Rakhman, I.; Moroz, N.; Basso, M.; Payappilly, J.; Kazakov, S.; Hernandez-Guzman, F.; Gaisina, I. N.; Kozikowski, A. P.; Ratan, R. R.; Gazaryan, I. G. Utilization of an In Vivo Reporter for High Throughput Identification of Branched Small Molecule Regulators of Hypoxic Adaptation. *Chem. Biol.* **2010**, *17* (4), 380−391.
(77) Neitemeier, S.; Dolga, A. M.; Honrath, B.; Karuppagounder, S. S.; Alim, I.; Ratan, R. R.; Culmsee, C. Inhibition of HIF-Prolyl-4-Hydroxylases Prevents Mitochondrial Impairment and Cell Death in a Model of Neuronal Oxytosis. *Cell Death Dis.* **2016**, *7* (5), e2214.
(78) Archana; Srivastava, V. K.; Kumar, A. Synthesis and Anticonvulsant Activity of 1-Acetyl-5-Arylidenyl-3-(2′-Oxo/Thio-Barbiturinyl)-2-Pyrazolines. *Arzneim. Forsch. Drug Res.* **2002**, *52* (11), 787−791.
(79) Gorovoy, A. S.; Guyader, D.; Lejon, T. Highly Efficient Synthesis of Trioxopyrimidine-Based Chalconoids Under Solvent-Free Conditions. *Synth. Commun.* **2014**, *44* (9), 1296−1300.
(80) Abdel Latif, N. A.; Batran, R. Z.; Khedr, M. A.; Abdalla, M. M. 3-Substituted-4-Hydroxycoumarin as a New Scaffold with Potent CDK Inhibition and Promising Anticancer Effect: Synthesis, Molecular Modeling and QSAR Studies. *Bioorg. Chem.* **2016**, *67*, 116−129.
(81) Thomsen, R.; Christensen, M. H. MolDock: A New Technique for High-Accuracy Molecular Docking. *J. Med. Chem.* **2006**, *49* (11), 3315−3321.

NOTE ADDED AFTER ISSUE PUBLICATION

Due to a production error, this paper was published in volume 5, issue 5, before the final corrections had been incorporated. Notably, on pages 362 and 369, the surname of the second author is corrected, from "Bogahawattha" to "Bogahawaththa", and an additional affiliation is given for the eighth author, Norio Suzuki: Applied Oxygen Physiology Project, New Industry Creation Hatchery Center (NICHe), Tohoku University, 2-1 Seiryo-machi, Aoba-ku, Sendai, Miyagi 980-8575, Japan. Additional changes are made in notations throughout the text, none of which has a significant impact on the scientific content or the conclusions of the paper. The online version of the original paper has been updated to reflect these final corrections. The revised version was published on the Web on June 9, 2022. An Addition/Correction was published in Volume 5, Issue 7.

https://doi.org/10.1021/acsptsci.2c00002
ACS Pharmacol. Transl. Sci. 2022, 5, 362−372